Chinese Journal of Natural Medicines

Korean red ginseng alleviates benign prostatic hyperplasia by dysregulating androgen receptor signaling and inhibiting DRP1–mediated mitochondrial fission

Geum–Lan HONG, Kyung–Hyun KIM, Sung–Pil CHO, Hui–Ju LEE, Yae–Ji KIM, Ju–Young JUNG

Citation: Geum–Lan HONG, Kyung–Hyun KIM, Sung–Pil CHO, Hui–Ju LEE, Yae–Ji KIM, Ju–Young JUNG, Korean red ginseng alleviates benign prostatic hyperplasia by dysregulating androgen receptor signaling and inhibiting DRP1–mediated mitochondrial fission, Chinese Journal of Natural Medicines, 2024, 22(7), 599–607. doi: 10.1016/S1875–5364(24)60619–9.

View online: https://doi.org/10.1016/S1875–5364(24)60619–9

Available online at www.sciencedirect.com
ScienceDirect
Chinese Journal of Natural Medicines 2024, **22**(7): 599-607
doi: 10.1016/S1875-5364(24)60619-9
Chinese Journal of Natural Medicines

•Original article•

Korean red ginseng alleviates benign prostatic hyperplasia by dysregulating androgen receptor signaling and inhibiting DRP1-mediated mitochondrial fission

HONG Geum-Lan[1, 2Δ], KIM Kyung-Hyun[1Δ], CHO Sung-Pil[1], LEE Hui-Ju[1], KIM Yae-Ji[1], JUNG Ju-Young[1*]

[1] *Department of Veterinary Medicine & Institute of Veterinary Science, Chungnam National University, Daejeon 34134, Korea;*
[2] *Department of Anatomy, College of Medicine, Konyang University, Daejeon 35365, Korea*

Available online 20 Jul., 2024

[ABSTRACT] *Panax ginseng* (C.A. Mey.) has been traditionally employed in Korea and China to alleviate fatigue and digestive disorders. In particular, Korean red ginseng (KRG), derived from streamed and dried *P. ginseng*, is known for its anti-aging and anti-inflammatory properties. However, its effects on benign prostatic hyperplasia (BPH), a representative aging-related disease, and the underlying mechanisms remain unclear. This study aims to elucidate the therapeutic effects of KRG on BPH, with a particular focus on mitochondrial dynamics, including fission and fusion processes. The effects of KRG on cell proliferation, apoptosis, and mitochondrial dynamics and morphology were evaluated in a rat model of testosterone propionate (TP)-induced BPH and TP-treated LNCaP cells, with mdivi-1 as a control. The results revealed that KRG treatment reduced the levels of androgen receptors (AR) and prostate-specific antigens in the BPH group. KRG inhibited cell proliferation by downregulating cyclin D and proliferating cell nuclear antigen (PCNA) levels, and it promoted apoptosis by increasing the ratio of B-cell lymphoma protein 2 (Bcl-2)-associated X protein (Bax) to Bcl-2 expression. Notably, KRG treatment enhanced the phosphorylation of dynamin-related protein 1 (DRP-1, serine 637) compared with that in the BPH group, which inhibited mitochondrial fission and led to mitochondrial elongation. This modulation of mitochondrial dynamics was associated with decreased cell proliferation and increased apoptosis. By dysregulating AR signaling and inhibiting mitochondrial fission through enhanced DRP-1 (ser637) phosphorylation, KRG effectively reduced cell proliferation and induced apoptosis. These findings suggest that KRG's regulation of mitochondrial dynamics offers a promising clinical approach for the treatment of BPH.

[KEY WORDS] Androgen; Benign prostatic hyperplasia; Fission; Korean red ginseng; Mitochondria
[CLC Number] R965 **[Document code]** A **[Article ID]** 2095-6975(2024)07-0599-09

Introduction

Benign prostatic hyperplasia (BPH) is the most common age-related prostate disease in older men, affecting up to 90% of men over 80 years old [1]. BPH is characterized by the hyperproliferation of prostatic epithelial and stromal cells, leading to prostate enlargement [2]. Although the precise etiology of BPH remains unclear, dihydrotestosterone (DHT), a male hormone converted from testosterone by 5α-reductase type 2, plays a central role. The binding of DHT to androgen receptors (ARs) activates androgen signaling, which affects cell proliferation and apoptosis [3]. The growth of prostate cells is maintained by a delicate balance between apoptosis and proliferation; disruption of this balance results in abnormal prostate cell growth and BPH [4].

LI *et al*. reported disrupted mitochondrial morphology and membrane potential in BPH [5]. Mitochondria are essential for maintaining cellular homeostasis through their various biological roles, such as ATP production, apoptosis, and fatty acid β-oxidation [6]. Mitochondrial activity is regulated by their morphology, which undergoes dynamic processes of fusion (elongation) and fission (shortening) [7]. Proper regulation of mitochondrial morphology is essential for maintaining energy supply and cellular homeostasis [8, 9]. Mitochondrial dysfunction has been implicated in various human diseases, such as cancer, diabetes, and aging-related diseases [10].

Korean red ginseng (KRG, *Panax ginseng* C. A. Mey) is a steamed and dried ginseng product traditionally used in

[Received on] 12-Feb.-2024
[Research funding] This work was supported by the 2021 Grant from the Korean Society of Ginseng.
[*Corresponding author] E-mail: jyjung@cnu.ac.kr
[Δ]These authors contributed equally to this work.
These authors have no conflict of interest to declare.

Korea and China for treating various conditions, including digestive issues, fatigue, and sore throat [11, 12]. Ginsenosides, the major components of ginseng, have diverse activities, including anti-inflammatory and anticancer effects [13, 14]. Some studies have reported that KRG exerts anti-aging effects [15, 16] and that *P. ginseng* prevents BPH progression [17, 18]. However, the specific effects of KRG on BPH are not well understood. Therefore, this study investigated the effects of KRG on testosterone propionate (TP)-induced BPH models. The results are anticipated to provide a theoretical foundation for developing KRG-based clinical strategies to mitigate BPH through the regulation of mitochondrial dynamics.

Materials and Methods

KRG

Red ginseng was produced from fresh *P. ginseng* roots by the Korea Ginseng Corporation (authentic sample; V21H002087, Buyeo, Chung-nam, Korea). The details of the experiments are described in Supplementary Information.

The constituents of KRG were analyzed by high-performance liquid chromatography (HPLC) with an Acquity UPLC system (Waters Co., Milford, MA, USA) equipped with a UV detector following the KRG in-house protocol [19]. The specific HPLC conditions are detailed in Table 1. HPLC analysis was performed for quality control of KRG, and representative chromatograms of the reference standard and KRG are shown in Fig 1. Standard ginsenoside materials were used for the analysis, revealing concentrations of ginsenoside Rb1 and Rg3s were 6.24 and 4.03 mg·g^{-1}, respectively. The composition of other sample constituents is provided in Supplementary File 1.

Animals and BPH model

Forty male 6-week-old Sprague-Dawley (SD) rats were purchased from Orient Bio (Seongnam, Korea). The rats were acclimated in a specific pathogen-free animal facility under controlled conditions (22 ± 2 °C, 55% ± 5% humidity) with standard chow and water provided *ad libitum*. All experimental procedures followed the *Guide for the Care and Use of Laboratory Animals* (National Institute of Health, Bethesda, MA, USA) and were approved by the animal ethics committee of Chungnam National University (Daejeon, Korea; 202103A-CNU-012). The rats were randomly assigned into the following groups (n = 8/group) according to their weights: control (corn oil without TP, s.c., and PBS 10 mg·kg^{-1}, p.o.), BPH (5mg·kg^{-1} TP in corn oil, s.c. and PBS 10 mg·kg^{-1}, p.o.), Fina (TP + finasteride 10 mg·kg^{-1} p.o.), KRG200 (TP + KRG 200 mg·kg^{-1}, p.o.), and KRG400 (TP + KRG 400 mg·kg^{-1}, p.o.). The BPH animal model was prepared as previously described [20]. Detailed experimental procedures are provided in Supplementary Information.

Table 1 Instrument and working conditions for the analysis of KRG using HPLC

HPLC analysis	
Column	UPLC Acquity BEH C_{18} (50 mm × 2.1 mm, 1.7 μm, Waters Co.)
Detector	UV detector (205nm)
Flow rate	0.6 mL·min^{-1}
Injection volume	2 μL
Solvent A	D.W
Solvent B	Acetonitrile
Gradient condition (%)/min	Solvent B (%)
0−0.5	15
14.5	30
15.5	32
18.5	38
24.0	43
27.0−31.0	55
33.0−38.0	90
38.1−43.0	15

Enzyme-linked immunosorbent assay (ELISA)

The concentrations of testosterone and DHT and the activity of 5α-reductase type 2 in serum and homogenized prostate samples were measured using commercial ELISA kits (MyBioSource, San Diego, CA, USA) according to the manufacturer's instructions.

Histological examination

Following euthanasia, prostate tissues were harvested, fixed in 10% formalin (Thermo Fisher Scientific, Waltham, MA, USA), embedded in paraffin, and cut into 4 μm-thick sections. After deparaffinization and dehydration, the sections were stained with hematoxylin (Agilent, Santa Clara, CA, USA) and eosin (Sigma-Aldrich) as previously described [20]. We imaged ten randomly selected fields for each stained section under a light microscope (Nikon Eclipse 80i, Nikon, Tokyo, Japan) at 200 × and 400 × magnifications. Epithelial thickness was measured using Image J software (Image J v1. 46a; NIH, USA).

Immunohistochemistry

Immunohistochemistry was performed following established laboratory protocols [20]. Briefly, sections were boiled in an antigen retrieval solution (Sigma-Aldrich) to enhance antigen expression. The sections were then treated with 3% hydrogen peroxide in methanol to block endogenous peroxidase activity and with 0.5% Triton X-100 (Sigma-Aldrich) for 30 min to permeabilize the cells. Normal goat serum was used to block non-specific binding sites. The sections were incubated with a primary antibody (anti-PCNA, 1 : 3000; Abcam, Cambridge, UK) at 4 °C overnight. The next day, the sections were incubated for 2 h with a secondary goat anti-rabbit antibody (1 : 200; Ab Frontier) and developed using 3,3-diaminobenzidine (DAB). Mayer's hematoxylin was used for counterstaining, and the sections were mounted with Canada balsam (Sigma Aldrich). Then randomly selected fields from each section were evaluated under an Eclipse 80i microscope Eclipse 80i microscope (Nikon) at 400 × magnification.

TUNEL staining

Apoptosis was assessed by TUNEL staining using a peroxidase *in situ* apoptosis detection kit (Merck, Darmstadt, Germany) according to the manufacturer's instructions and

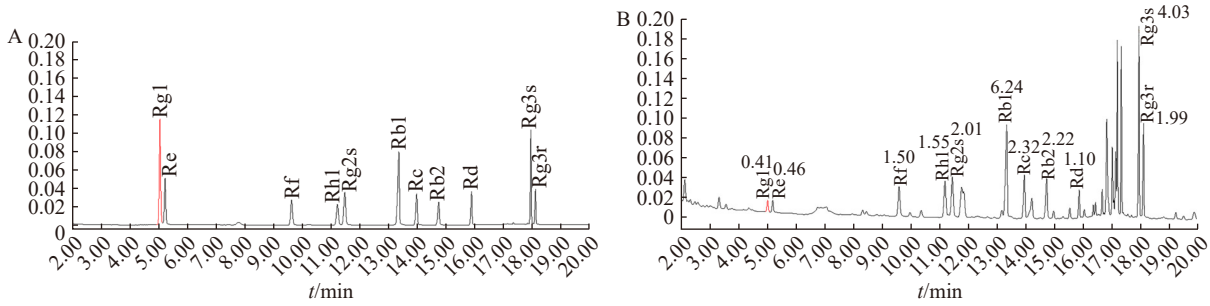

Fig. 1 Representative HPLC chromatograms of KRG.

our laboratory protocols. We imaged ten random fields for each brown stained section under a light microscope (Eclipse 80i) at 200 × and 400 × magnifications and measured the proportion of apoptosis-positive cells per 100 prostate cells.

Western blotting analysis

Proteins were extracted and quantified using a bicinchoninic acid assay (Thermo Fisher Scientific). The extracted proteins were separated on 8%−15% SDS-polyacrylamide gels and transferred onto polyvinylidene fluoride membranes. The membranes were blocked with 5% skim milk in 1 × PBS containing Tween-20 (PBS-T) for 2 h and then incubated with a primary antibody at 4 °C overnight (Supplementary File S2). After washing with PBS-T, the membranes were incubated with secondary goat anti-rabbit and goat anti-mouse IgG antibodies (1 ∶ 5000, AbFrontier) at room temperature for 2 h. The proteins were visualized using an enhanced chemiluminescence detection kit (Bio-Rad, Hercules, CA, USA) with a chemiluminescence LuminoGraph III Lite (ATTO, Tokyo, Japan) and quantified using a CS analyzer (ATTO).

Immunofluorescence analysis

For immunofluorescence analysis, 4 μm-thick tissue sections were processed up to the primary antibody treatment, as previously described. The sections were then incubated with the primary antibodies against translocase of outer mitochondrial membrane 20 (Tom20, Santa Cruz) and phosphorylated dynamin-related protein 1 (p-DRP1, ABclonal) at 4 °C overnight. After incubation, the slides were washed with PBS-T and incubated with secondary antibodies, goat anti-rabbit Alexa Fluor 488 (1 ∶ 100) and anti-mouse Alexa Fluor 594 (1 ∶ 100), for 2 h in a humid chamber at room temperature. Human prostate adenocarcinoma LNCaP cells (ATCC, Manassas, VA, USA) were seeded onto eight-chamber slides and treated with TP in combination with Fina, KRG, or mdivi-1, a quinazolinone that selectively inhibits the association of DRP1 with mitochondria and prevents mitochondrial fission [21, 22]. After 72 h, the slides were treated with 25 nmol·L^{-1} MitoTracker solution (Invitrogen) for 10 min. Following MitoTracker staining, the cells were fixed with 4% paraformaldehyde and rinsed several times with buffer. Both the prostate tissues and LNCaP cells were then treated with ProLong™ Gold Antifade Mountant with DAPI (Invitrogen) for nuclear staining. Images were obtained with an LSM 880 Airyscan confocal microscope (Zeiss, Jena, Germany) and analyzed with DP Controller software (Olympus, Tokyo, Japan) and Image J (NIH). At least five randomly selected images were captured and analyzed to assess mitochondrial structure. After image optimization, the relative mitochondrial size in each cell was measured using particle analysis.

Cell culture

After evaluating that KRG is not toxic to LNCaP cells (Supplementary Materials and Methods), LNCaP cells were cultured in RPMI-1640 medium (Gibco, NY, USA) supplemented with 5% FBS (Gibco) and 100 mg·mL^{-1} penicillin/streptomycin (Gibco) to examine the regulatory effects of KRG, nonsaponin-KRG (NS-RG), and saponin-KRG (S-RG) on androgen signaling and mitochondrial dynamics. The cells were seeded into six-well plates (1 × 10^5 cells/well) and cultured for 24 h in phenol red-free RPMI medium. Subsequently, cells were treated with 1 μmol·L^{-1} TP except for the control cells. The cells were co-treated with TP and either finasteride (10 μmol·L^{-1}), KRG (200 and 400 μg·mL^{-1}), or NS-RG/S-RG (200 mg·mL^{-1}) for 72 h. After incubation, cells were washed twice with PBS and prepared for protein extractions. To inhibit DRP-1 expression, the cells were pretreated with 50 mmol·L^{-1} mdivi-1 (Sigma-Aldrich) for 6 h before TP treatment.

ANNEXIN-V/propidium iodide double staining flow cytometry

We analyzed the changes in apoptosis using a FITC annexin V apoptosis detection kit (BioLegend, San Diego, CA, USA) with propidium iodide (PI). Following treatment and washing, FITC Annexin V and PI solutions were added to the cells, and apoptosis was analyzed using a flow cytometer (FACS Canto II, 488 nm; BD Biosciences, San Jose, CA, USA).

Statistical analysis

All experiments were conducted in a double-blinded manner. Data were randomly selected and expressed as the mean ± standard deviation (SD) of two experiments. GraphPad Prism 5.0 (GraphPad Software, La Jolla, CA, USA) was used for all data analyses. Nonparametric data were analyzed using the Mann-Whitney U test, with the Tukey test for multiple comparisons where relevant. Statistical significance was set at a P value < 0.05.

Results

KRG inhibits prostate growth in TP-induced BPH rat

The BPH group exhibited significantly larger and heavier prostates than the control group (P < 0.001, Fig. 2A,

Table 2). Treatment with KRG, which showed no toxicity (Supplementary File S3), resulted in reduced prostate weight and size in a dose-dependent manner ($P < 0.001$). Histopathological analysis confirmed the decrease in prostate growth in the KRG-treated group (Fig. 2B). In the BPH group, epithelial and stromal cells showed higher proliferation rates, with epithelial cells undergoing a transition from squamous to columnar morphology. The epithelial thickness in the BPH group was three times greater than that in the control group ($P < 0.001$). In contrast, both epithelial and stromal cell proliferation rates, as well as epithelial thickness, were significantly reduced in the Fina and KRG groups, with epithelial thickness reduced by half (Fig. 2C). These findings suggested that KRG inhibits prostate enlargement.

Androgen signaling in TP-induced BPH rats

The BPH group had more than double the serum and tissue levels of testosterone and DHT than did the control group. However, both testosterone and DHT levels were lower in the Fina and KRG groups than in the BPH group (Figs. 3A and 3B). Although KRG reduced hormone levels, it did not significantly reduce testosterone or DHT levels in blood or tissues. However, the levels of AR and prostate-specific antigen (PSA) were effectively reduced in the KRG groups compared with those in the BPH group (Fig. 3C).

Apoptosis and proliferation in TP-induced BPH rats

Cyclin D expression was higher in the BPH group than in the control group (Fig. 4A), but it was significantly lower in the Fina and KRG groups ($P < 0.001$ and $P < 0.01$, respectively). Similarly, the number of proliferating cell nuclear antigen (PCNA)-positive cells was higher in the BPH group than in the control group ($P < 0.001$), whereas it was lower in the Fina and KRG groups ($P < 0.001$ and $P < 0.01$, respectively; Fig. 4B). The degree of apoptosis contrasted that of cell proliferation, as shown in Figs. 4A and 4C. The ratio of Bax/Bcl-2 was lower in the BPH group than in the control group, but it increased in the Fina and KRG groups. Notably, the expression of Bcl-2, an anti-apoptotic protein, was significantly higher in the BPH group but decreased after

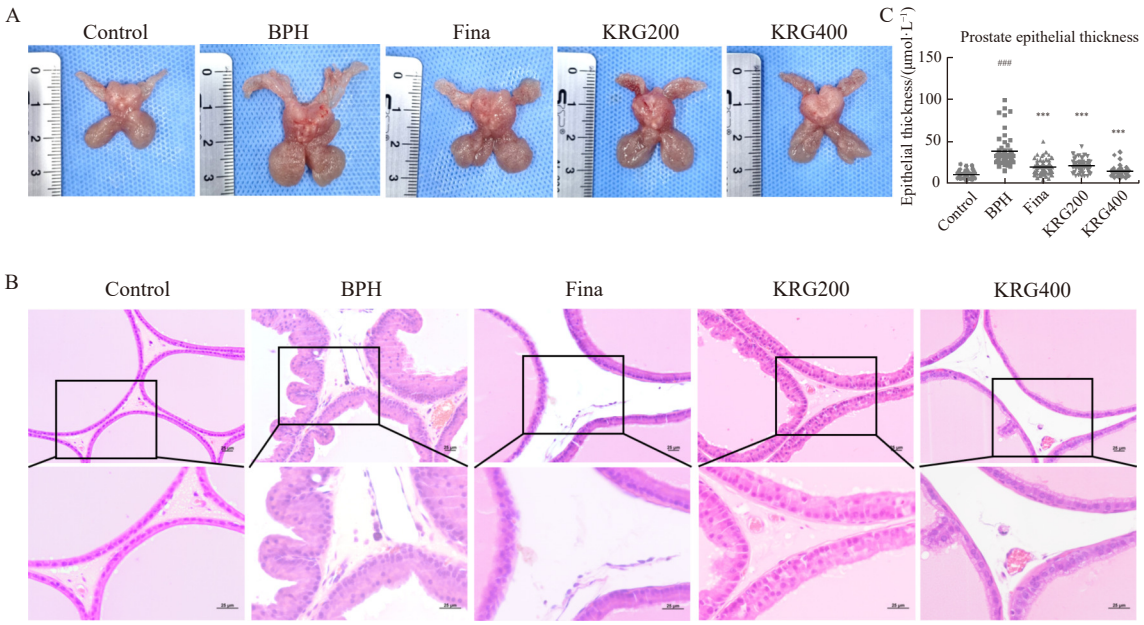

Fig. 2 Effects of KRG on prostate size and histopathological changes determined by hematoxylin and eosin staining (Scale bar = 25 μm). BPH rat models were established through daily subcutaneous injection of TP (5 mg·kg^{-1}) for 28 d. (A) Prostate tissue. (B) Histopathological changes (first line: 200 ×, second line: 400 ×). (C) Prostate epithelial thickness was increased in the BPH group and decreased in the Fina and KRG groups. Control: PBS; BPH: TP; Fina: TP + finasteride (10 mg·kg^{-1}, p.o.); KRG200: TP + KRG (200 mg·kg^{-1}, p.o.); KRG400: TP + KRG (400 mg·kg^{-1}, p.o.). Data are presented as the mean ± SD (n = 8/group). $^{###}P < 0.001$ *vs* Control; $^{***}P < 0.001$ *vs* BPH.

Table 2 Effects of KRG on body and prostate weights (Mean ± SEM, n = 8)

	Body weight (g)	Prostate weight (g)	
		Absolute	Relative
Control	426.175 ± 9.036	1.361 ± 0.0556	0.319 ± 0.0106
BPH	400.913 ± 4.217	2.360 ± 0.0742$^{###}$	0.589 ± 0.0198$^{###}$
Fina	410.988 ± 12.989	2.013 ± 0.0460**	0.495 ± 0.0240**
KRG200	425.400 ± 9.497	2.129 ± 0.0571	0.502 ± 0.0152*
KRG400	417.929 ± 7.085	2.009 ± 0.0634*	0.482 ± 0.0195**

$^{###}P < 0.001$ *vs* Control; $^{*}P < 0.05$, $^{**}P < 0.01$ *vs* BPH.

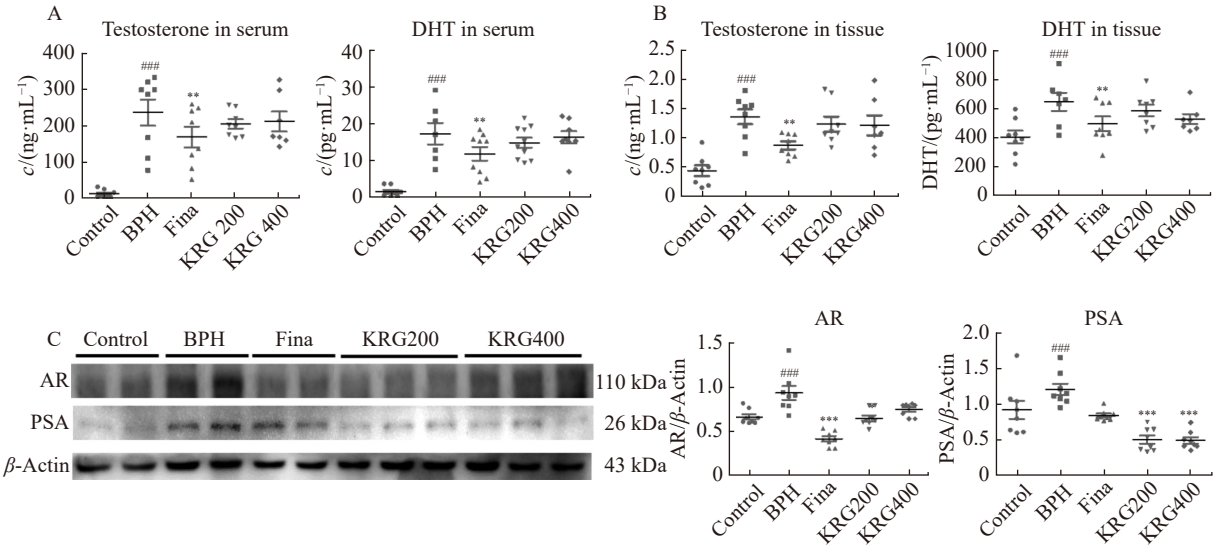

Fig. 3 Effects of KRG on DHT and testosterone concentrations in serum and prostate tissue, and AR and PSA expressions in prostate tissue. (A) Concentrations of DHT and T in serum. (B) Concentrations of DHT and T in tissue. (C) Western blotting analysis of AR and PSA expressions in rat prostate, and densitometry estimates were normalized to those of *β*-actin. Control: PBS; BPH: TP; Fina: TP + Finasteride (10 mg·kg^{-1}, p.o.); KRG200: TP + KRG (200 mg·kg^{-1}, p.o.); KRG400: TP + KRG (400 mg·kg^{-1}, p.o.). Data are expressed as the mean ± SD (n = 8/group). $^{###}P < 0.001$ *vs* Control; $^{*}P < 0.05$, $^{**}P < 0.01$, and $^{***}P < 0.001$ *vs* BPH.

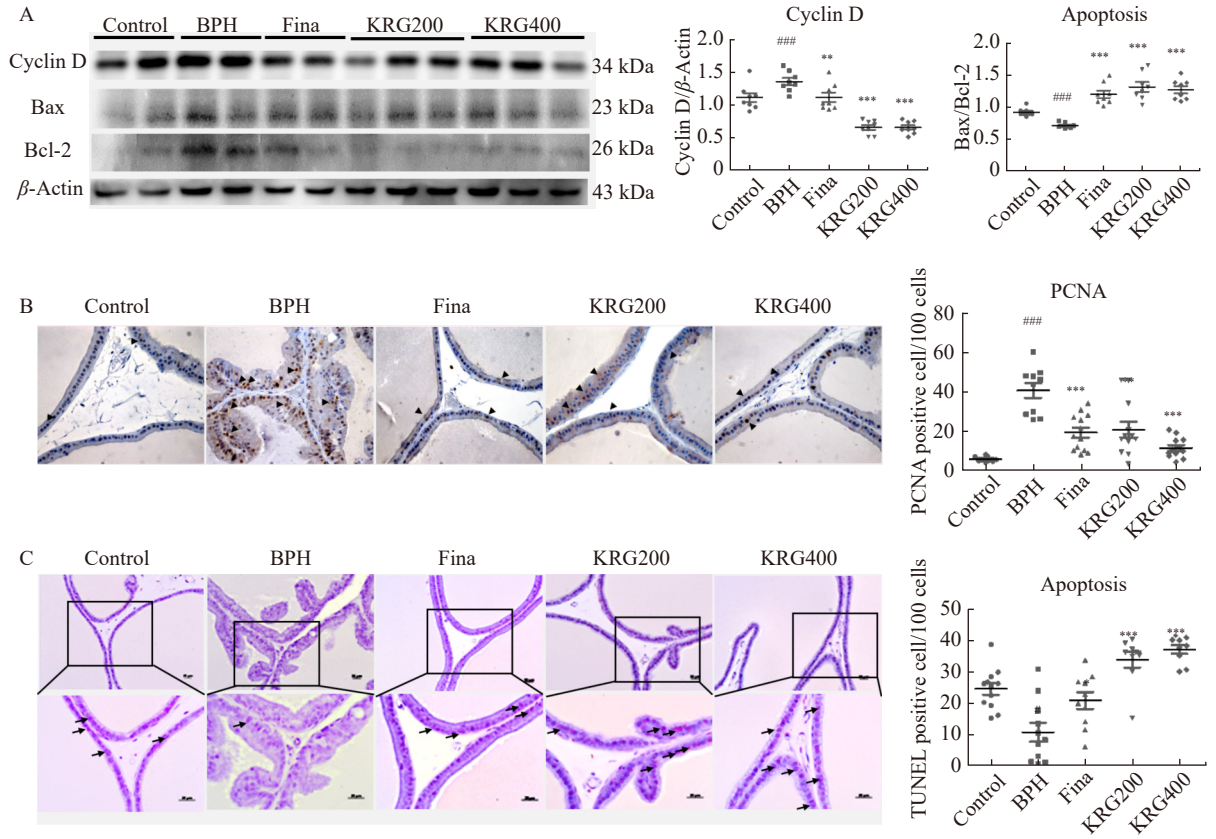

Fig. 4 Effects of KRG on proliferation and apoptosis in prostate tissue. (A) Western blotting analysis of cyclin D, Bax, and Bcl-2 expressions. The densitometry estimates were normalized to those of *β*-actin and the Bax/Bcl-2 ratio. (B) Immunohistochemistry of PCNA; arrowheads indicate positive-stained nuclei in epithelial cells. (C) TUNEL staining; arrows indicate positive cells per 100 prostate cells. Control: PBS; BPH: TP; Fina: TP + Finasteride (10 mg·kg^{-1}, p.o.); KRG200: TP + KRG (200 mg·kg^{-1}, p.o.); KRG400: TP + KRG (400 mg·kg^{-1}, p.o.). Data are expressed as mean ± SD (n = 8/group). $^{#}P < 0.05$, and $^{###}P < 0.001$ *vs* Control; $^{*}P < 0.05$, $^{**}P < 0.01$, and $^{***}P < 0.001$ *vs* BPH.

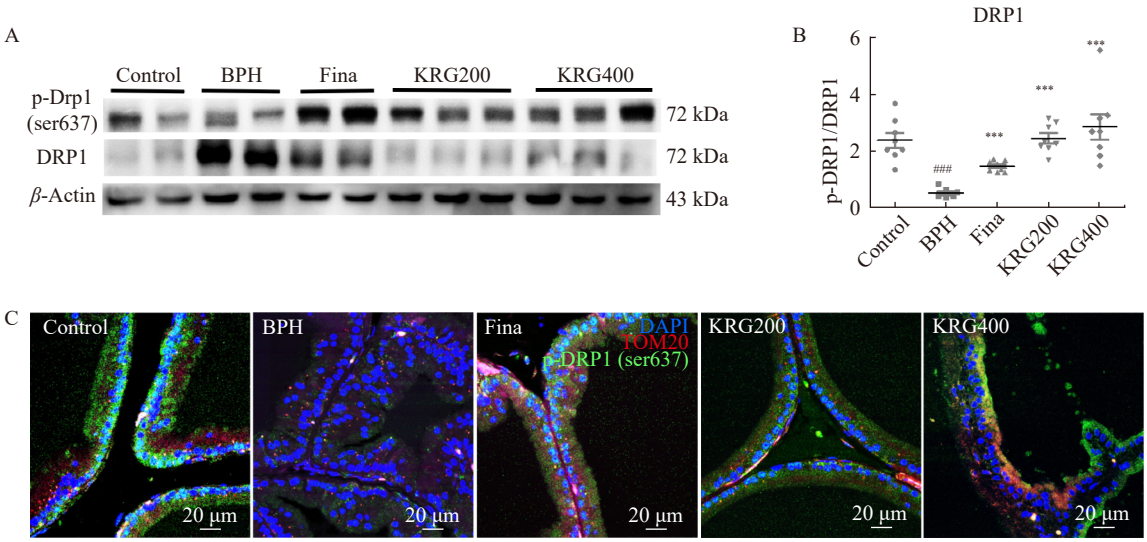

Fig. 5 Effects of KRG on DRP1 expression in prostate tissue. (A, B) Western blotting analysis of p-DRP1 (ser637), normalized to those of DRP1. (C) Representative confocal images of double immunofluorescence staining for p-DRP1 (ser637, green), TOM20 (red), and nuclei (DAPI, blue). Control: PBS; BPH: TP; Fina: TP + Finasteride (10 mg·kg^{-1}, p.o.); KRG200: TP + KRG (200 mg·kg^{-1}, p.o.); KRG400: TP + KRG (400 mg·kg^{-1}, p.o.). Data are expressed as the mean ± SD (n = 8/group). $^{\#}P < 0.05$, and $^{\#\#\#}P < 0.001$ *vs* Control; $^{*}P < 0.05$, $^{**}P < 0.01$, and $^{***}P < 0.001$ *vs* BPH.

KRG treatment. The number of TUNEL-positive cells was lower in the BPH group than in the control group ($P < 0.05$) but significantly higher in the Fina and KRG groups ($P < 0.05$ and $P < 0.001$, respectively, Fig. 4C). These findings suggest that KRG disrupts androgen signaling by dysregulating AR expression, thereby inhibiting proliferation and promoting apoptosis.

Mitochondrial dynamics in TP-induced BPH rats

The expression of p-DRP1 (ser 637) was lower in the BPH group than in the control group, whereas it was higher in the Fina and KRG groups ($P < 0.001$, Fig. 5A). As shown in Fig. 5C, double immunofluorescence staining for p-DRP1 and TOM20, an outer mitochondrial membrane protein used as a marker of mitochondrial mass [23], revealed reduced intensity in the BPH group compared with that in the control group. However, treatment with KRG induced the cytosolic expression of p-DRP1, increasing the intensity of positively stained cells increased in the Fina and KRG groups. In the KRG400 group, the green fluorescence of p-DRP1 appeared separately from that of TOM20, whereas p-DRP1 and TOM20 were colocalized in the BPH group, representing mixed colors. These results indicated that KRG enhances the phosphorylation of DRP1, inhibiting mitochondrial fission and promoting mitochondrial elongation.

KRG reduces mitochondrial fission by phosphorylating DRP-1 in TP-treated LNCaP cells

We investigated the effects of TP-induced BPH on androgen signaling and mitochondrial dynamics in TP-induced androgenic prostate epithelial cells. Compared with those in the control cells, the levels of AR and PSA were higher in the TP-treated cells, which showed no cytotoxicity ($P < 0.01$, Fig. 6, Supplementary File S4). However, AR and PSA levels were significantly lower in 400 mg·mL^{-1} KRG-treated cells than in TP-treated cells. In contrast, the expression of p-DRP1 increased in TP-treated cells, especially in those treated with Fina and KRG. Cyclin D expression was significantly higher in TP-treated cells ($P < 0.001$), but this increase was mitigated in Fina- and KRG-treated cells ($P < 0.05$ and $P < 0.001$, respectively). Inhibition of DRP1 activity by mdivi-1 further reduced cyclin D expression by 20% compared to TP-treated cells. The Bax/Bcl-2 ratio increased due to decreased Bcl-2 expression in KRG and mdivi-1 treated cells ($P < 0.001$). Flow cytometric analysis confirmed the apoptotic effects of KRG, showing an increase in annexin V-positive/PI-negative cells in KRG-treated cells compared with TP-treated cells, indicating early apoptosis (Fig. 6C). Mitochondrial morphology was also altered with treatment. In TP-treated cells, mitochondria appeared as smaller, separated cytosolic particles, whereas in Fina- and KRG-treated cells, mitochondria were more connected and elongated. Mdivi-1-treated cells similarly displayed more elongated and connected mitochondria. The relative mitochondrial particle size, reduced in TP-treated cells compared with control cells, increased fivefold in Fina- and KRG-treated cells (Fig. 6D). These results suggested that KRG suppressed prostate cell proliferation and induced apoptosis by inhibiting mitochondrial fission.

Effects of S-RG and NS-RG on BPH in testosterone-treated LNCaP cells

We compared the activities of the KRG components BPH, S-RG, and NS-RG in TP-treated LNCaP cells. AR expression was lower in both S-RG and NS-RG-treated cells than in TP-treated cells; however, the expression of PSA was considerably lower in S-RG-treated cells ($P < 0.001$). Notably, the expression of p-DRP-1 (ser 637) was higher in S-RG-treated cells, whereas no changes were observed in NS-

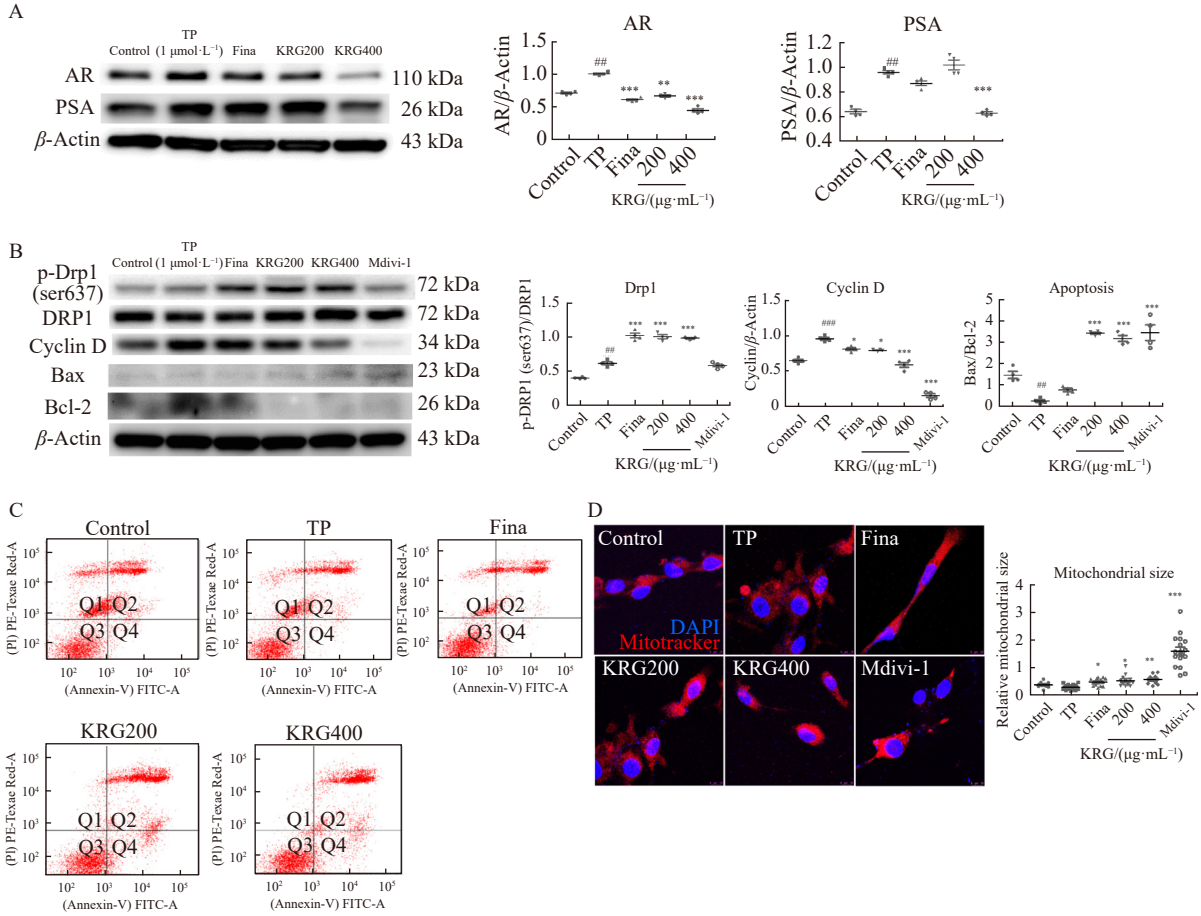

Fig. 6 Effects of KRG in testosterone-treated LNCaP cells. LNCaP cells were treated with Fina or KRG (200 or 400 μg·mL^{-1}). Western blotting analysis of total cell lysates for (A) AR, PSA, (B) Drp1, Cyclin D, Bax, and Bcl-2 expressions. (C) Fluorescence microscopy images showing the cellular distribution of the mitochondria-specific dye MitoTracker Deep Red (Red) and DAPI (blue) as well as (D) relative mitochondrial size. Data are expressed as the mean ± SD (n = 4/group). $^{\#}P < 0.05$, $^{\#\#}P < 0.01$, and $^{\#\#\#}P < 0.001$ *vs* Control; $^{*}P < 0.05$, $^{**}P < 0.01$, and $^{***}P < 0.001$ *vs* TP.

RG cells. The Bax/Bcl-2 ratio was higher in S-RG-treated cells ($P < 0.05$, Fig. 7). In summary, KRG inhibited mitochondrial fission and effectively alleviated BPH *via* the action of the saponin components.

Discussion

KRG has traditionally been used to prevent and alleviate various age-related conditions, including obesity, diabetes, and dyslipidemia [24]. Numerous studies have documented the efficacy of ginseng in managing BPH [17, 25]. Bae *et al*. reported that red ginseng and 20(*S*)-Rg3 alleviated BPH by dysregulating AR expression [26]. In this study, we explored the effects of KRG on mitochondrial dynamics regulation and found that KRG mitigates BPH by reducing mitochondrial fission, which in turn induces apoptosis and decreases cell proliferation.

Prostate size and weight are critical indicators of BPH severity [27]. Our study showed that TP treatment significantly increased prostate weight, size, and epithelial thickness. Conversely, KRG treatment significantly reduced these parameters. TP treatment also elevated PSA levels along with T, DHT, and AR levels. While KRG did not affect T or DHT concentrations, it effectively reduced AR and PSA levels, indicating a disruption of AR signaling. Previous studies have shown that red ginseng can downregulate AR expression by degrading its protein structure [26]. Androgen signaling, which is activated by the interaction of androgens with AR, promotes increased cell proliferation and decreased apoptosis [28]. Consistent with the disruption of androgen signaling by KRG, our study observed reduced cell proliferation in KRG-treated groups, evidenced by decreased levels of cyclin D and PCNA. Additionally, TUNEL staining revealed increased apoptosis in KRG-treated groups, indicated by a higher Bax/Bcl-2 ratio. Collectively, these results indicated that KRG inhibits prostate cancer cell proliferation and promotes apoptosis in TP-induced BPH *via* AR dysregulation.

Mitochondrial dynamics−the reversible process of fission and fusion [29]−play an important role in maintaining mitochondrial homeostasis and functionality, particularly under cellular stress. An imbalance in these processes can lead to mitochondrial dysfunction and impaired energy metabolism, potentially resulting in severe conditions such as seizures and stroke [30, 31]. Dysregulation of mitochondrial dynamics has been implicated in numerous diseases, including Parkinson's

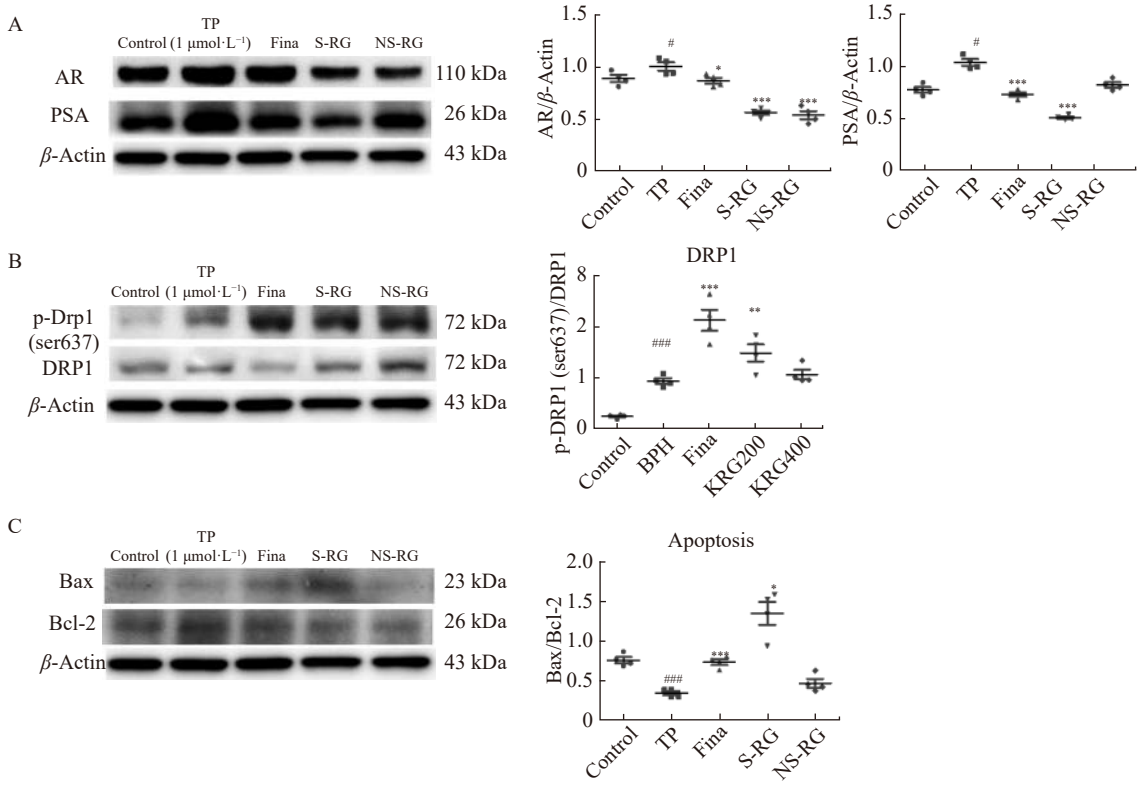

Fig. 7 Effects of S-RG and NS-RG on testosterone-treated LNCaP cells. LNCaP cells were treated with Fina, S-RG (200 μg·mL^{-1}) or NS-RG (200 μg·mL^{-1}). Western blotting analysis of total cell lysates for (A) AR, PSA, (B) Drp1, (C) Bax, and Bcl-2 expression. Data are expressed as the mean ± SEM (n = 4/group). $^{\#}P < 0.05$, and $^{\#\#\#}P < 0.001$ *vs* Control; $^{*}P < 0.05$, $^{**}P < 0.01$, and $^{***}P < 0.001$ *vs* TP.

disease, lung cancer, and melanoma, making the artificial regulation of mitochondrial dynamics a promising therapeutic approach [32-34]. Recent studies have shown that androgens induce the expression of DRP1, a key regulatory protein involved in mitochondrial conformational changes [35] and proliferation in prostate cancer [36]. The impact of DRP1 on mitochondrial fission is modulated by its phosphorylation status. Phosphorylation of DRP1 at ser 579 and ser 616 can promote mitochondrial fission [37], whereas the phosphorylation of DRP1 at ser 656 and ser 637 inhibits mitochondrial fission, causing DRP1 to remain in the cytoplasm rather than being recruited to mitochondria [38]. In our study, androgen signaling reduced levels of p-DRP1 (ser 637). Interestingly, p-DRP1 (ser 637) levels were significantly higher in the KRG-treated group than in the BPH group. Immunostaining revealed increased cytoplasmic expression of p-DRP1 (ser 637) following KRG treatment, suggesting that KRG inhibits mitochondrial fission. For further investigation, we examined mitochondrial fission in epithelial cells treated with TP, KRG, or mdivi-1 (a DRP1 inhibitor). MitoTracker staining indicated that mitochondrial particles were small and dispersed after TP treatment. In contrast, KRG and mdivi-1 treatments resulted in larger, elongated mitochondrial particles, indicating inhibited mitochondrial fission. These findings suggest that KRG inhibits mitochondrial fission by activating the phosphorylation of DRP1 (ser 637).

Our results showed that the inhibition of mitochondrial fission was not associated with reduced cell death but rather with the suppression of cell proliferation. Recent evidence indicates that the activation of mitochondrial fission is involved in apoptosis [39]. We found that fission was inhibited by KRG treatment, although early apoptosis was induced based on the Bax/Bcl-2 ratio and flow cytometry results. This apoptotic effect of KRG was further confirmed by treatment with the mitochondrial fission inhibitor mdivi-1, which also reduced cell proliferation and induced apoptosis.

We also examined the effects of different KRG components, specifically S-RG and NS-RG, on mitochondrial fission. Our findings revealed that S-RG activated the phosphorylation of DRP1 at serine 637, leading to apoptosis. Thus, S-RG effectively inhibits mitochondrial fission by phosphorylating DRP1 at serine 637 and likely plays a crucial role in KRG-induced suppression of mitochondrial fission, thereby alleviating BPH.

One limitation of the current study is that we focused solely on the effects of KRG on BPH without evaluating its reproductive toxicity. Previous studies, such as those by Traish, have reported that reduced sperm count is a side effect of finasteride in both treated rats and human patients [40]. Although we confirmed that KRG is not toxic to the spleen, liver, and kidneys, its safety concerning reproductive toxicity needs to be investigated in future studies.

Conclusion

In conclusion, KRG dysregulates AR signaling, resulting in the inhibition of mitochondrial fission through the

phosphorylation of DRP1 at serine 637. This action effectively reduces cell proliferation and induces apoptosis, primarily due to the saponin components of KRG. Our findings provide a robust empirical foundation for developing KRG-based clinical strategies to regulate mitochondrial dynamics and alleviate BPH.

References

[1] Berry SJ, Coffey DS, Walsh PC, *et al*. The development of human benign prostatic hyperplasia with age [J]. *J Urol*, 1984, **132**(3): 474-479.

[2] Lee KL, Peehl DM. Molecular and cellular pathogenesis of benign prostatic hyperplasia [J]. *J Urol*, 2004, **172**(5 Pt 1): 1784-1791.

[3] Carson C, Rittmaster R. The role of dihydrotestosterone in benign prostatic hyperplasia [J]. *Urology*, 2003, **61**(4 Suppl 1): 2-7.

[4] Kyprianou N, Tu H, Jacobs SC. Apoptotic versus proliferative activities in human benign prostatic hyperplasia [J]. *Hum Pathol*, 1996, **27**(7): 668-675.

[5] Li Y, Wang Q, Li J, *et al*. SIRT3 affects mitochondrial metabolic reprogramming *via* the AMPK-PGC-1alpha axis in the development of benign prostatic hyperplasia [J]. *Prostate*, 2021, **81**(15): 1135-1148.

[6] Archer SL. Mitochondrial dynamics: mitochondrial fission and fusion in human diseases [J]. *N Engl J Med*, 2013, **369**(23): 2236-2251.

[7] Hall AR, Burke N, Dongworth RK, *et al*. Mitochondrial fusion and fission proteins: novel therapeutic targets for combating cardiovascular disease [J]. *Br J Pharmacol*, 2014, **171**(8): 1890-1906.

[8] Tilokani L, Nagashima S, Paupe V, *et al*. Mitochondrial dynamics: overview of molecular mechanisms [J]. *Essays Biochem*, 2018, **62**(3): 341-360.

[9] Yu R, Lendahl U, Nistér M, *et al*. Regulation of mammalian mitochondrial dynamics: opportunities and challenges [J]. *Front Endocrinol (Lausanne)*, 2020, **11**: 374.

[10] Lee HC, Wei YH. Mitochondria and aging [J]. *Adv Exp Med Biol*, 2012, **942**: 311-327.

[11] Jun H. *Donguibogam* [M]. Jinhan M&B: 2020.

[12] Liu CX, Xiao PG. Recent advances on ginseng research in China [J]. *J Ethnopharmacol*, 1992, **36**(1): 27-38.

[13] Jeong YA, Kim BR, Kim DY, *et al*. Korean red ginseng extract increases apoptosis by activation of the noxa pathway in colorectal cancer [J]. *Nutrients*, 2019, **11**(9): 2026.

[14] Baek KS, Yi YS, Son YJ, *et al*. *In vitro* and *in vivo* anti-inflammatory activities of Korean red ginseng-derived components [J]. *J Ginseng Res*, 2016, **40**(4): 437-444.

[15] Shin KK, Yi YS, Kim JK, *et al*. Korean red ginseng plays an anti-aging role by modulating expression of aging-related genes and immune cell subsets [J]. *Molecules*, 2020, **25**(7): 1492.

[16] Shin SJ, Nam Y, Park YH, *et al*. Therapeutic effects of non-saponin fraction with rich polysaccharide from Korean red ginseng on aging and Alzheimer's disease [J]. *Free Radic Biol Med*, 2021, **164**: 233-248.

[17] Park HK, Kim SK, Lee SW, *et al*. A herbal formula, comprising *Panax ginseng* and bee-pollen, inhibits development of testosterone-induced benign prostatic hyperplasia in male Wistar rats [J]. *Saudi J Biol Sci*, 2017, **24**(7): 1555-1561.

[18] Kim SK, Chung JH, Lee BC, *et al*. Influence of *Panax ginseng* on alpha-adrenergic receptor of benign prostatic hyperplasia [J]. *Int Neurourol J*, 2014, **18**(4): 179-186.

[19] Bae BS, Lee MW, Lee JS, *et al*. Comparison of the constituents of processed Korean and American ginseng grown in Korea siz years [J]. *Korean J Med Crop Sci*, 2021, **29**(1): 35-44.

[20] Hong GL, Park SR, Jung DY, *et al*. The therapeutic effects of *Stauntonia hexaphylla* in benign prostate hyperplasia are mediated by the regulation of androgen receptors and 5 alpha-reductase type 2 [J]. *J Ethnopharmacol*, 2020, **250**: 112446.

[21] Smith G, Gallo G. To mdivi-1 or not to mdivi-1: is that the question [J]. *Dev Neurobiol*, 2017, **77**(11): 1260-1268.

[22] Manczak M, Kandimalla R, Yin X, *et al*. Mitochondrial division inhibitor 1 reduces dynamin-related protein 1 and mitochondrial fission activity [J]. *Hum Mol Genet*, 2019, **28**(2): 177-199.

[23] Schleiff E, Turnbull JL. Functional and structural properties of the mitochondrial outer membrane receptor Tom20 [J]. *Biochemistry*, 1998, **37**(38): 13043-13051.

[24] Yin J, Zhang H, Ye J. Traditional Chinese medicine in treatment of metabolic syndrome [J]. *Endocr Metab Immune Disord Drug Targets*, 2008, **8**(2): 99-111.

[25] Lee JY, Kim S, Kim S, *et al*. Effects of red ginseng oil (KGC11o) on testosterone-propionate-induced benign prostatic hyperplasia [J]. *J Ginseng Res*, 2022, **46**(3): 473-480.

[26] Bae JS, Park HS, Park JW, *et al*. Red ginseng and 20(*S*)-Rg3 control testosterone-induced prostate hyperplasia by deregulating androgen receptor signaling [J]. *J Nat Med*, 2012, **66**(3): 476-485.

[27] Cornu JN, Oelke M, Parsons KF. Benign prostatic hyperplasia and lower urinary tract symptoms [J]. *N Engl J Med*, 2012, **367**(17): 1668.

[28] Isaacs JT, Isaacs WB. Androgen receptor outwits prostate cancer drugs [J]. *Nat Med*, 2004, **10**(1): 26-27.

[29] Youle RJ, van-der Bliek AM. Mitochondrial fission, fusion, and stress [J]. *Science*, 2012, **337**(6098): 1062-1065.

[30] Chen H, Chomyn A, Chan DC. Disruption of fusion results in mitochondrial heterogeneity and dysfunction [J]. *J Biol Chem*, 2005, **280**(28): 26185-26192.

[31] Hu C, Huang Y, Li L. Drp1-dependent mitochondrial fission plays critical roles in physiological and pathological progresses in mammals [J]. *Int J Mol Sci*, 2017, **18**(1): 144.

[32] Dal YF, Kim SH, Ding Z, *et al*. Mitochondrial dynamic alterations regulate melanoma cell progression [J]. *J Cell Biochem*, 2019, **120**(2): 2098-2108.

[33] Lennon FE, Salgia R. Mitochondrial dynamics: biology and therapy in lung cancer [J]. *Expert Opin Investig Drugs*, 2014, **23**(5): 675-692.

[34] Bastian P, Dulski J, Roszmann A, *et al*. Regulation of mitochondrial dynamics in Parkinson's disease: is 2-methoxyestradiol a missing piece [J]. *Antioxidants (Basel)*, 2021, **10**(2): 248.

[35] Smirnova E, Griparic L, Shurland DL, *et al*. Dynamin-related protein Drp1 is required for mitochondrial division in mammalian cells [J]. *Mol Biol Cell*, 2001, **12**(8): 2245-2256.

[36] Lee YG, Nam Y, Shin KJ, *et al*. Androgen-induced expression of DRP1 regulates mitochondrial metabolic reprogramming in prostate cancer [J]. *Cancer Lett*, 2020, **471**: 72-87.

[37] Prieto J, León M, Ponsoda X, *et al*. Early ERK1/2 activation promotes DRP1-dependent mitochondrial fission necessary for cell reprogramming [J]. *Nat Commun*, 2016, **7**: 11124.

[38] Cribbs JT, Strack S. Reversible phosphorylation of Drp1 by cyclic AMP-dependent protein kinase and calcineurin regulates mitochondrial fission and cell death [J]. *EMBO Rep*, 2007, **8**(10): 939-944.

[39] Youle RJ, Karbowski M. Mitochondrial fission in apoptosis [J]. *Nat Rev Mol Cell Biol*, 2005, **6**(8): 657-663.

[40] Traish AM. Negative impact of testosterone deficiency and 5alpha-reductase inhibitors therapy on metabolic and sexual function in men [J]. *Adv Exp Med Biol*, 2017, **1043**: 473-526.

Cite this article as: HONG Geum-Lan, KIM Kyung-Hyun, CHO Sung-Pil, *et al*. Korean red ginseng alleviates benign prostatic hyperplasia by dysregulating androgen receptor signaling and inhibiting DRP1-mediated mitochondrial fission [J]. *Chin J Nat Med*, 2024, **22**(7): 599-607.